

Contents lists available at ScienceDirect

Journal of Catalysis

journal homepage: www.elsevier.com/locate/jcat





Shifts in catalyst deactivation mechanisms as a function of surface coverage during Friedel-Crafts acylation in zeolites

Ismaeel Alalq, Huy Nguyen-Phu, Steven Crossley

School of Sustainable Chemical, Biological, and Materials Engineering, University of Oklahoma, Norman, OK 73019, USA

ARTICLE INFO

Keywords: Zeolites Direct acylation Deactivation 2-methyfuran Acetic acid

ABSTRACT

The production of commodity chemicals from renewable resources is often accompanied by rapid catalyst deactivation rates. An important example is direct Friedel Crafts acylation, which can yield a range of valuable products from surfactants to renewable transportation fuels. Furanic acyl acceptors are among the most intriguing and promising possible acceptors; however, they undergo self-coupling reactions in the presence of Brønsted acid surface sites leading to rapid catalyst deactivation. In this contribution, we study 2-methylfuran acylation with acetic acid over HZSM-5 catalysts at temperatures ranging from 160 to 240 °C, revealing the remarkable shift in deactivation behavior as a function of surface coverage of acetic acid. We reveal that a surface saturated with acetic acid lowers the deactivation rate by blocking the direct access of furanic species to surface sites. However, on surfaces fully saturated with carboxylic acids, deactivation is revealed to proceed via reactions between adsorbed products with gas phase methylfuran reactants.

1. Introduction

Friedel-Crafts acylation is an important and attractive process for the formation of C—C bonds with renewable feedstocks. Products of this reaction are typically commodity chemicals such as fragrances, surfactants, and renewable fuels [1]. This reaction involves an acylating agent such as acyl chloride and an acyl acceptor, which usually consists of aromatic or heteroaromatic rings. The traditionally common catalyst for this reaction is aluminum trichloride (AlCl₃) [2]. This catalyst, however, produces large amounts of waste, which detrimentally influence the economic and environmental impact of this chemistry [3].

In contrast, upgrading biomass-derived chemicals via the direct acylation of heteroaromatics with carboxylic acids over zeolite catalysts can enable more renewable and sustainable routes toward producing valuable chemicals while minimizing waste and improving efficiency. The acylation of 2-methyfurans directly over zeolites has been reported both with acetic acid (AA) [4] and with larger organic acids/anhydrides [5] to produce fuels and high value chemicals. The prospective use of acylation chemistry to yield fuels is potentially more carbon efficient resulting in higher overall efficiency and resulting lifecycle energy return on investment when compared with other more common catalytic upgrading approaches that lose some C to light gas phase biproducts such as ketonization [6-8].

Further advancement in acylation chemistry requires advancement in our understanding of not only the chemistry occurring on the zeolite surface that influences reaction rates, but also the aspects that lead to catalyst deactivation. A variety of carboxylic acids found in biomass-derived streams could serve as promising acylating agents, while promising acyl acceptor candidates include cellulose and hemicellulose derived furanics [4] and lignin-derived phenolics [5,9,10], both of which represent common platform molecules from biomass [4,11-17] and are typically better acyl acceptors than unfunctionalized aromatics. While many advancements have been made in recent years regarding improved understanding of acylation mechanisms on the catalyst surface with these renewable precursors, much less is understood regarding the side reactions that occur in parallel and ultimately lead to catalyst deactivation.

Furanic species, while appealing as acyl acceptors, have a tendency to cause catalyst deactivation when in contact with Brønsted zeolites. Recent reports have shown that this deactivation can be significantly influenced by the concentration of furanics in the feed, and the surface coverage of carboxylic acids that limit direct interactions of furanics with the Brønsted sites on the zeolite surface [4,14]. The well-known propensity to form coke when furanic species are in direct contact with acid sites on the catalyst suggests that this is the primary factor of consideration when improving catalyst stability. However, at high

E-mail address: stevencrossley@ou.edu (S. Crossley).

^{*} Corresponding author.

coverage of carboxylic acids, deactivation still persists via an unknown mechanism. This work aims to clarify the pathways responsible for deactivation under these regimes, allowing for further improvements in yields and stability.

In this manuscript, the reason for catalyst deactivation during the acylation of 2-methylfuran (2-MF) with acetic acid (AA) over HZSM-5 zeolites is evaluated over clean and acid saturated surfaces. We show how each reactant and product species influences deactivation rates via controlled independent introduction of each compound under a wide range of conditions. Rates of active site loss are quantified, clarifying the underlying cause of catalyst deactivation. Further insight is attained by introducing toluene, which due to its diminished rates as an acyl acceptor serves as a strongly binding site inhibitor under these conditions. Modifying toluene partial pressure, as well as manipulation of acid site density via selective exchange of active sites, allows us to evaluate the role of sequential reactions along the diffusion path within the zeolite crystallites under reaction conditions.

2. Experimental section

2.1. Chemicals and materials

The HZSM-5 catalysts sample used in this study are commercial grade obtained Zeolyst international (CBV2314 Si/Al = 11.5, CBV 5524G Si/Al = 25, CBV8014 Si/Al = 40, and CBV28014 Si/Al = 140). These samples were received in the ammonium-ion form and calcined to obtain the proton form. The calcination was carried out in a 1 in. quartz tube under air flow of 100 standard cubic centimeters per minute (SCCM) and heated inside an oven at ramp rate of 2 $^{\circ}\text{C/min}$ to 600 $^{\circ}\text{C}$ then kept for 5 h. CBV8014 Si/Al = 40 catalyst was employed in most reactions while other catalyst samples will be noted when used. The sodium exchanged sample (Na-ZSM-5) was obtained by partially titrating Brønsted acid sites (BAS) in CBV28014 Si/Al = 140. This was prepared by adding 2 g of CBV28014 in a 40 mL 0.004 M NaNO3 solution under stirring at 700 rpm for 30 min at room temperature then washed and filtered five times. The collected sample was dried and calcined using the same procedure mentioned earlier. The acylating agent is acetic acid (glacial, ACS reagent, ≥99.7 %, Sigma-Aldrich). The acyl acceptor is 2-Methylfuran (98+ %, stab., Alfa Aesar). Toluene (ACS reagent, \geq 99.5 %, Sigma-Aldrich) was added as non-reactive adsorbant in some cases to manipulate the surface coverage of the catalyst. The carrier gas used for the experiments was nitrogen (ultra high purity GD 5.0). The trace levels of the stabilizer butylated hydroxytoluene present in purchased 2-Methylfuran was removed via distillation prior to use as a reactant.

2.2. Catalyst characterization

2.2.1. IPA-TPRx measurements

Isopropylamine temperature-programmed reaction (IPA-TPRx) was used to quantify Brønsted acid site density in the catalyst samples. Catalyst samples were packed in a 1/4-inch quartz tube and then pretreated under helium flow of 30 mL/min heated at 10 °C/min to 300 °C and held for 1 h. The temperature was then reduced to 100 °C. Catalyst samples were exposed to several 2µL IPA pulses to saturate the Brønsted acid sites thoroughly, then allowed the helium to flow for 1 h to remove the physiosorbed or weakly adsorbed IPA. The TPRx started by ramping the temperature from 10 °C/min to 600 °C. The evolution of desorbed species was continuously monitored by a Cirrus mass spectrometer (MKS) recording the following signals m/z=17 and (NH₃), 44 (IPA), and 41 (propylene). The Brønsted acid site density was quantified by calibrating the MS signals using the average of several 0.5 mL-pulses of propylene.

2.2.2. Pore volume measurements

The micropore volume of fresh and spent catalyst samples were evaluated by the T-plot method. Nitrogen adsorption analysis was implemented on a Micromeritics ASAP 2020 at liquid nitrogen temperature (-196 $^{\circ}\text{C}$). Catalyst samples were degassed at 350 $^{\circ}\text{C}$ with a heating rate of 5 $^{\circ}\text{C/min}$ in vacuum pressure for 10 h to remove physiosorbed moisture and volatile impurities. The weight of the dried sample after degassing was measured and corrected. Then, the sample was cooled down to -196 $^{\circ}\text{C}$ for nitrogen adsorption analysis.

2.2.3. IR spectroscopy

The retained species on the surface of the spent HZSM-5 catalyst has been analyzed using infrared spectroscopy in a PerkinElmer Spectrum 100 FT-IR Spectrometer equipped with Harrick Praying Mantis chamber. The background was measured using KBr (FT-IR grade, $\geq 99\,\%$ trace metals basis) from Sigma Aldrich. The spent catalyst was placed on top of a layer of KBR to reduce sample thickness and increase signal during diffuse reflectance. The spent catalyst was heated at a ramp rate of $10\,^{\circ}\text{C}$ to temperatures $160\,^{\circ}\text{C}$, $200\,^{\circ}\text{C}$, $240\,^{\circ}\text{C}$ and $300\,^{\circ}\text{C}$ under flowing helium at rate of $50\,$ mL/min where $64\,$ scans has been performed for each temperature to track the evolution of the spectra of the spent catalyst. Then, the temperature was cooled down to $160\,^{\circ}\text{C}$ (the usual reaction temperature) to observe the spectra region of the retained species (hard coke) after removal of the soft coke by helium sweeping.

2.2.4. Pyroprobe system

Retained surface species (soft coke) was analyzed using a CDS Analytical Pyroprobe 5250 T. Spent catalyst sample (ranging between 2 mg and 3 mg) was loaded into a fire polished quartz tube (CDS Analytical, 10A1-3015). A filler rod (CDS Analytical, 10A1-3016S) was inserted within the quartz tube to seal the bottom. a small amount of quartz wool (CDS Analytical, 0100-9014) is placed on top of the filler rod where the spent catalyst sample rests. The sample tubes are sent via autosampler to a platinum coil jacket which it is heated rapidly to temperatures between 300 and 500C and held for 5 min. Concurrently, a sweeping flow of helium gas at 14 mL/min directly carries out the vapor of the desorbed species from the spent catalyst and then sent to a GC–MS (Shimadzu QP2010S + GC/MS-FID system). The GC–MS is equipped with a 60 m semi-polar Restek RTX-1701 column with thickness and diameter of 0.25 μ m and 0.25 mm.

2.2.5. Thermogravimetric analysis

Thermogravimetric analysis (TGA) was performed on a Netzsch STA 449F1 equipped with a pin thermocouple and a Netzsch nano balance to quantify the amount of coke formed on the spent HZSM-5 catalyst sample during acylation reactions. After the reaction, N_2 sweeping at 125 mL/min was employed on spent catalyst at ramp rate of 10 °C/min to 500 °C for 1 h to remove the soft coke and accurately account for the hard coke. Then, temperature program oxidation (TPO) was carried out under flowing air (50 mL/min). The spent catalyst sample was heated from room temperature up to 600 °C at the ramp rate of 10 °C/min, held at 600 °C for 30 min and then cooled down to the original temperature of 40 °C. The coke on the sample was determined by the weight loss of the sample after the TPO experiment.

2.3. Catalytic reaction

The acylation of 2-MF with AA over HZSM-5 zeolites was carried out in the gas phase in a fixed bed tubular reactor. A measured amount of catalyst between 4 and 100 mg mixed with glass beads packed between quartz wool in a 1/4-inch quartz reactor tube was then pretreated at $10\,^{\circ}$ C/min to $300\,^{\circ}$ C and held for 1 h under flowing nitrogen to remove physiosorbed moisture then cooled down to reaction temperature ($160\,^{\circ}$ C in most cases). The nitrogen carrier gas was set at $125\,$ SCCM and

adjusted, respectively, to maintain constant partial pressure of 2-MF (fed at 0.1 mL/hr via a liquid phase syringe). Reactions carried out with AA under 1st order reaction conditions were performed at an AA flowrate between 0.05 and 0.15 mL/hr in a room temperature liquid syringe, while AA was fed at flow rate between 1 and 2 mL/hr when operating in the 0th order regime with respect to AA. W/F values, defined as catalyst mass(g)/cumulative flow of AA + 2-MF(g), varied from 0.0044(h) at a reaction temperature of 160 °C, and 0.0035(h) at 240 °C unless otherwise noted. No detectable gas phase reaction products were observed under our reaction conditions aside from the acylation product reported. The reactor temperature was controlled via an attached thermocouple to the external surface of the reactor tube aligned with the center of the catalyst bed. After the catalyst pretreatment, the temperature was set to the desired reaction temperature and, the reactant feed rate was controlled using syringe pumps. The reactor outlet streamline was heated to 250 °C to avoid condensation of leaving species. A micro electric actuator controlled the six-port valve used to send the sample to an inline connected gas chromatograph Agilent 7890B equipped with a flame ionization detector and Zebron Phase: ZB-WAX (L imes ID imes thickness = 30 m \times 0.25 mm \times 0.25 μ m) column for separation of molecules in this reaction. The samples were collected from a glass trap connected to the vent line and products identified via Shimadzu GCMS-OP2010S. The reactant's response factor was achieved by flowing the reactant at the desired rate through a glass beads bed to mimic the catalyst bed, while the product response factor was attained by injection of standards. These response factors are used for further data analysis, such as conversion and carbon balance. The values for turnover frequency (TOF) were obtained using the following equation: -.

$$TOF = \frac{Moles \ of \ product \ formed \ per \ gram \ of \ catalyst}{Moles \ of \ Brønsted \ acid \ sites \ per \ gram \ of \ fresh \ catalyst} (1/s)$$

We emphasize here that the TOF references the number of active sites in the catalyst prior to introduction of the reactant. Thus the loss in what is referred to as TOF as a function of time is actually a reduction in the number of accessible active sites. Thus, if TOF is reported it is to facilitate an easier comparison between catalyst samples with varying site density. The dimensionless turnover number (TON) was calculated by integration of the turnover frequency with respect to time on stream using Equation (2): -.

$$TON = \int_{0}^{t} TOF(t)dt \tag{2}$$

All conversion levels of the limiting reactant 2-MF were maintained at under 10 % unless explicitly mentioned and estimated using the following equation: -.

saturated conditions at modest pressures. Operating under these conditions also facilitates avoidance of thermodynamic and diffusion limitations that would corrupt the kinetic data that is obtained [18]. All rates reported here are far from thermodynamic equilibrium values, as verified by increasing the catalyst loading as shown in Figure S1a. This conversion level of 37 % with the limiting reactant (2MF) results in an equilibrium constant obtained at 160 °C of 0.014 as defined by Equation (4).

$$K = \frac{(Acylation\ product)^*(H_2O)}{(2 - methylfuran)^*(acetic\ acid)} \tag{4}$$

This equilibrium constant is remarkably similar to the equilibrium constant obtained based upon the overall Gibbs free energy of reaction at 250 $^{\circ}$ C of 4.5 kcal/mol reported recently for the same reaction by Chen et al. [17], which translates to an equilibrium constant of 0.013 obtained via Equation (5).

$$K = exp\left(\frac{-\Delta G}{RT}\right) \tag{5}$$

Other groups [14] have recently reported even higher equilibrium constants for this reaction, implying that the conditions we are reporting here are all far from corruption due to approaching thermodynamic equilibrium values.

As mentioned in the section 2, all experiments were performed at conversion levels of the limiting reactant 2-MF of 10 % or below unless otherwise noted. The only exceptions are the experiments carried out at 240 °C with AA partial pressures ranging between 40 and 60 Torr, as lower conversion levels could not be obtained while maintaining a sufficient catalyst bed size. Under these conditions, the conversion of 2-MF was 23 %. We note that under these conditions, the reaction is still far from the equilibrium conversion of 44 % (Figure S1b), which translates to an equilibrium constant of 0.023 at this temperature.

In order to confirm that the rates reported here are not controlled by internal or external diffusion to the active sites, various HZSM-5 catalysts with different Brønsted acid site (BAS) densities (CBV2314 Si/Al = 11.5, CBV 5524G Si/Al = 25, CBV8014 Si/Al = 40, and CBV28014 Si/Al = 140) were employed. This is following the Koros-Nowak criteria, [19] later elaborated upon by Madon-Boudard [20], which presumes that by altering active site density within a catalyst particle, without modifying the nature of the particle or active site itself, one may compare turnover frequencies to assess the importance of diffusion corruptions to the data. It is clear from these results that over the Si/Al = 140 catalyst, internal diffusion does not limit reaction rates as shown in Fig. 1. We acknowledge that this conclusion presumes that the activity per site is identical for each of these catalysts, which carry varying Si/Al ratios. It is

$$methyl furan \ conversion = \frac{Moles \ of \ acylated \ product \ formed \ per \ hour}{Moles \ of \ 2 - methyl furan \ fed \ per \ hour} (mol\%)$$

The initial reaction rates were obtained by extrapolation to zero time on stream and used to accurately evaluate the catalyst deactivation during acylation.

3. Results and discussion

3.1. Assessment of kinetic rates

The acylation of 2-MF with AA over HZSM-5 occurs at temperatures as low as 160 $^{\circ}\text{C}$ to yield acetyl-methylfuran (Ac-MF) isomers and water. We note that these temperatures are considerably lower than those used in most acylation studies, which is an attempt to readily achieve acid

generally accepted that the acid strength of various Brønsted sites resulting from Al incorporation within zeolites are approximately the same. However, we acknowledge that the presence of more proximate acid sites, varying site location, or sites with extra lattice Al species may perturb reaction rates [21-23]. Therefore, by taking the lowest acid site density catalyst (Si/Al = 140) and performing Na exchange and carrying out the reaction under significantly higher temperatures (240 $^{\circ}$ C) where the role of diffusion is more likely to impact rates, one observes that identical turnover frequencies result. This suggests that the MFI 140 catalyst is clearly not corrupted by diffusion under these reaction conditions. The slightly elevated TOF observed with Si/Al = 40 when compared with Si/Al = 140, in spite of the higher acid site density of the

(3)

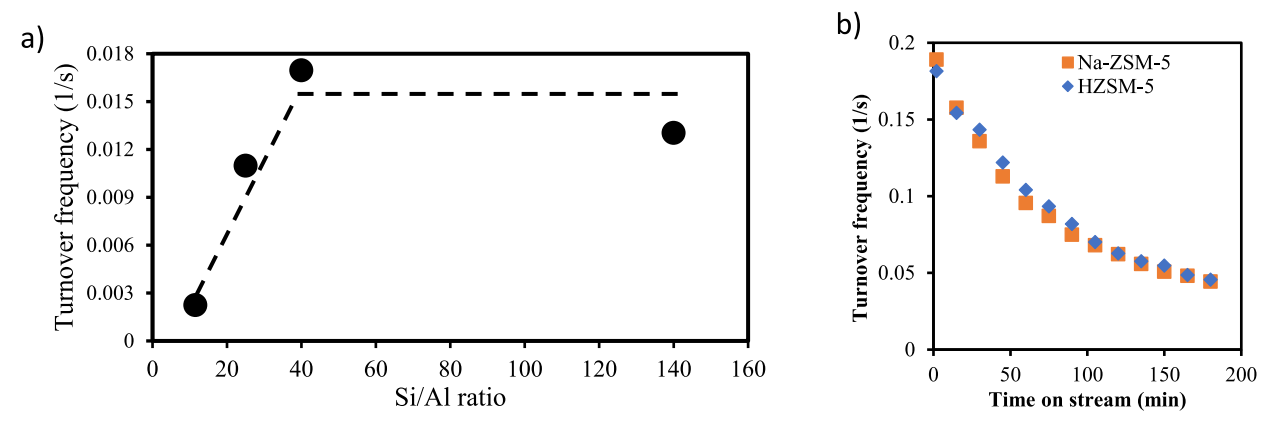


Fig. 1. a) Testing diffusion and reaction on HZSM-5 catalyst samples with different Si/Al ratios. CBV2314 Si/Al = 11.5, CBV 5524G Si/Al = 25, CBV8014 Si/Al = 40, and CBV28014 Si/Al = 140) at 160 °C after catalyst pretreatment at 300 °C for 1 h to remove the physiosorbed water. $PP_{AA} = 40$ Torr, $PP_{2.MF} = 2.6$ Torr. Lines are to guide the eye. b) Loss of BAS activity for Na titrated Na-ZSM-5 (25 % of BAS exchanged) and parent HZSM-5 both with (Si/Al = 140) at T = 240 °C with $P_{AA} = 40$ torr, $P_{2.MF} = 2.6$ torr.

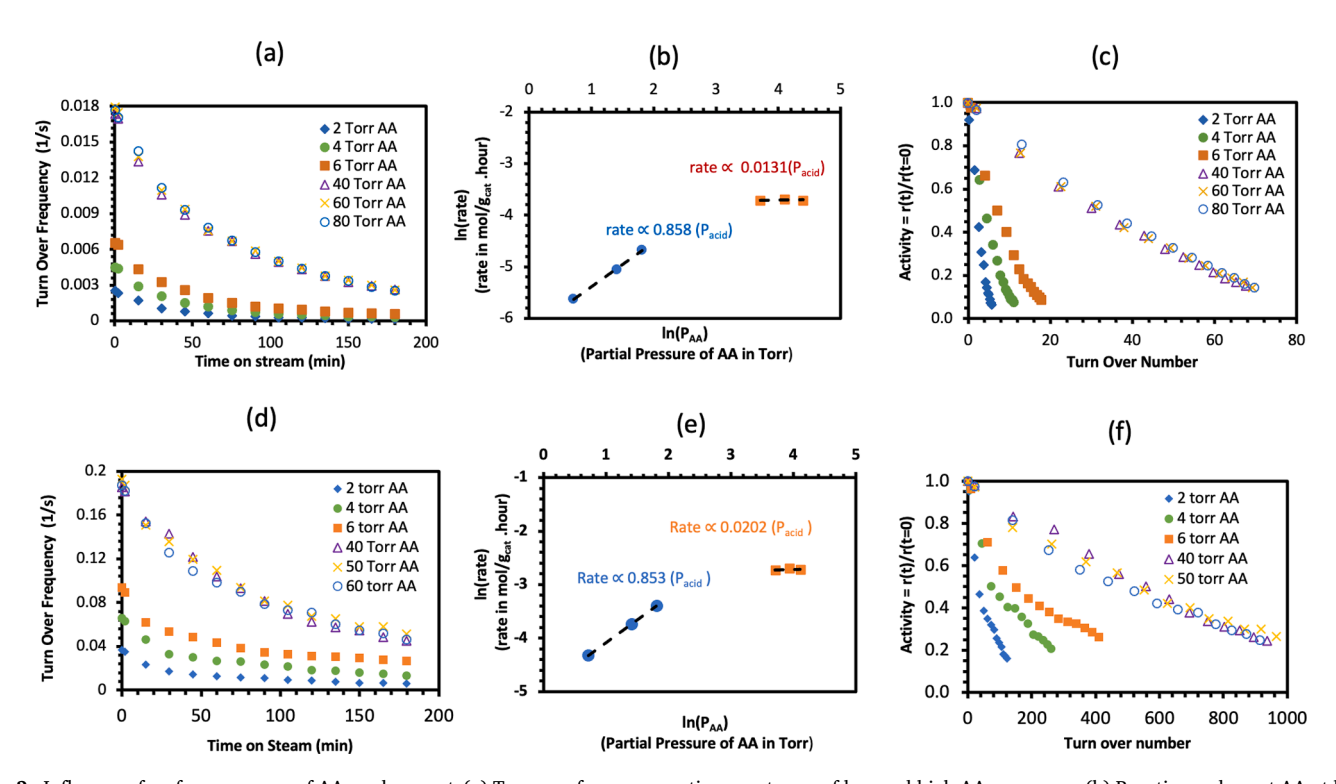


Fig. 2. Influence of surface coverage of AA on decay rate(a) Turnover frequency vs time on stream of low and high AA coverages. (b) Reaction order wrt AA at low and high coverages of AA. (c) Catalyst activity vs turnover number at low and high coverage AA. Results in (a), (b), and (c) obtained from reaction on HZSM-5 (Si/Al = 40) at 160 °C. Data in (d), (e), and (f) was collected from reaction on HZSM-5 (Si/Al = 140) at 240 °C. In order to maintain low conversion upon changing partial pressures, W/F values in a,b, and c range from 0.034(h) to 0.0023(h), W/F values in d,e,f range from 0.028 to 0.0024.

former, could be attributed to modest enhancements in rate due to the other factors described above (site location, proximity, or extra lattice species).

3.2. Role of surface coverage of AA

Catalyst deactivation can inherently be assessed under conditions that are limited by the rate of the reaction on the catalyst surface. Fig. 2 a and c reveal that the reaction rate steadily declines with time on stream across a wide range of acetic acid partial pressures. The rate of activity loss is indeed a strong function of acetic acid coverage, which as depicted in Fig. 2b spans from nearly first order at low AA partial pressures (2–6 Torr) to 0th order at high pressure (40–80 Torr). Fig. 2c

clearly demonstrates that the loss in activity is far less pronounced at higher acid coverage (higher AA partial pressure), as has been observed in prior studies [4,14,24], but deactivation persists. While the direct interaction of 2-MF with the Brønsted sites on the zeolite [4,14,24] have been proposed as the main cause of activity loss at low acid coverage, there is an alternative and unexplored deactivation mechanism that becomes prevalent under high coverage conditions. To ensure that operating at lower temperatures does not lead to any experimental artifacts such as reactant or product condensation within the pores that would otherwise corrupt this analysis, we conducted the same reaction at elevated temperature of 240 °C and observed similar deactivation behavior with respect to AA surface coverage as presented in Fig. 2 d, e, and f.

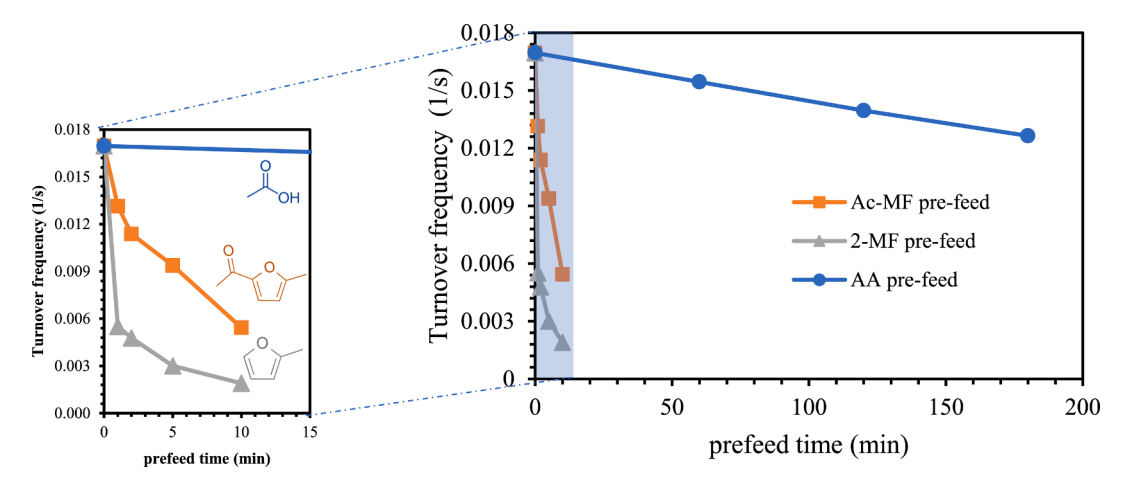


Fig. 3. (\triangle) Comparing initial active site loss resulting from the introduction of 2-MF for 1,2,5, and 10 min prior to adding the other reactant (AA) to the feed to start the reaction. (\blacksquare) Comparing initial active site loss resulting from the introduction of the product (Ac-MF) for 1,2,5, and 10 min prior to adding the reactants to the feed to start the reaction. (\blacksquare) Comparing initial active site loss resulting from the introduction of AA for 60,120, and 180 min prior to adding the other reactant (2-MF) to the feed to start the reaction. All reactions run on HZSM-5 (Si/Al = 40) at 160 °C after catalyst pretreatment at 300 °C for 1 h to remove the physiosorbed water. PP_{AA} = 40 Torr, PP_{2-MF} = 2.6 Torr. Molar flow rates during prefeed for both 2-MF and Ac-MF are equal.

3.3. Deactivation due to contact with individual species

To decouple the severity of each contributing species on deactivation rates, each species was fed independently for a certain period before introducing both reactants. By pre-introducing the acyl acceptor (2-MF), acylated product (Ac-MF), and acylating agent (AA) independently prior to introducing all reactants, one can discern the independent deactivation rates posed by each over a bare catalyst surface at $160~^{\circ}\text{C}$ over HZSM-5 (Si/Al = 40).

Fig. 3 shows that pre-feeding 2-MF for only 1 min led a loss of more than 67 % the initial catalytic activity. This illustrates the potential of methylfuran to severely form coke over a bare catalyst surface, even at moderate temperatures. It has been previously reported that that 2-MF can form dimers and trimers through hydration/dehydration and self-coupling on BAS [13] as illustrated in Fig. 4, eventually yielding species that are unable to desorb from the catalyst surface. While 2-MF has often been proposed as a main cause of deactivation [25-27], these results illustrate just how rapidly it can deactivate Brønsted sites.

Introducing the product Ac-MF, followed by a purge in inert gas prior to introducing acetic acid and measuring reaction rates, also results in rapid activity losses. The Ac-MF was pre-fed at a rate equimolar to 2-MF. Interestingly, the rate of deactivation due to product self-coupling

reactions appears to be less rapid than those observed upon injection of 2-MF alone, as shown in Fig. 3. The rapid deactivation rates observed are in agreement with previous reports where the acylated product was proposed as a coke precursor [12].

Exposure of only acetic acid is known to yield both acyl species and ketenes, but the contribution of these species to deactivation under these conditions is minimal. This is evident in Fig. 3, where pre-feeding AA for extended periods of time results in much lower rates of activity loss when contrasted with the other pre-fed molecules. The losses reported are likely due to reactions with the formed ketenes that are produced in low concentrations [28].

While the very distinct contributions to catalyst deactivation shown in Fig. 3 are obvious upon exposure to a bare catalyst surface, it is helpful to compare these results with those when both reactants are fed simultaneously in Fig. 2. Deactivation rates in all cases when acetic acid is co-fed along with 2-MF are dramatically reduced when contrasted with 2-MF or product introduced to the catalyst alone. However, the rate of catalyst deactivation in Fig. 2 upon co-introduction of reactants is still significantly larger than those observed in Fig. 3 upon exposure to acid alone. This implies that ketenes resulting from surface acyl species, or ketones formed from acid self-coupling are not the main sources of deactivation under these reaction conditions.

$$(1) \qquad (2) \qquad (4) \qquad (4)$$

Fig. 4. Reaction of (1) 2-MF on BAS forming (2) dimers through dehydration then self-coupling or hydration then ring opening to (3) 4-oxopentanal followed by dehydration and self-coupling to form (4) trimers.[13].

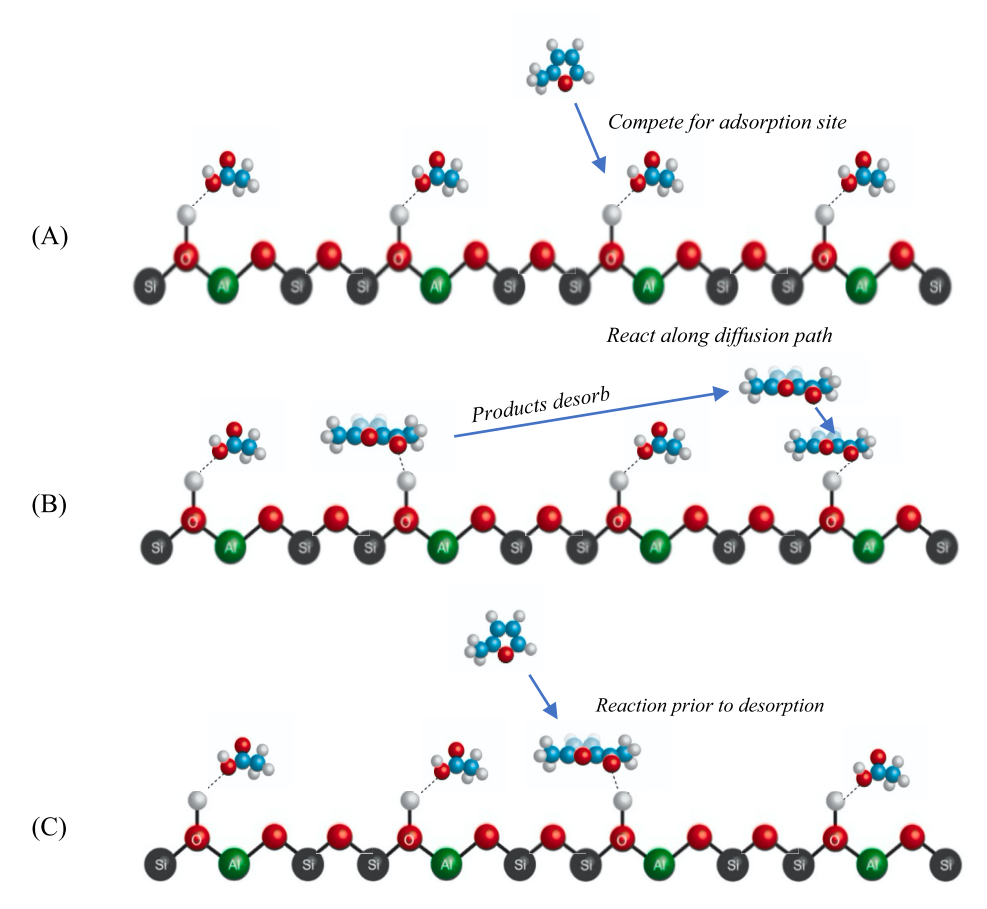


Fig. 5. Proposed cause of deactivation. (A) 2-MF compete with adsorbed acetic acid. (B) Product re-adsorption along the diffusion path. (C) sequential reaction of product prior to desorption.

3.4. Modification of available surface sites to investigate deactivation pathways

Because it is known that both the product Ac-MF and the feed 2-MF rapidly deactivate the catalyst when exposed to Brønsted acid sites, the underlying cause of deactivation can result from a variety of potential pathways. The three most likely deactivation pathways are depicted in Fig. 5. The simplest explanation (scenario A) is the competitive adsorption of the coke forming agent (2-MF) with acetic acid, where the adsorbed 2-MF is rapidly activated and further reacts with gas phase 2-MF species to yield larger species that do not leave the surface and ultimately deactivate said active sites, such as those depicted in Fig. 4. Deactivation rates following this pathway would be dictated by the ability of 2-MF to compete for surface sites. A graphical representation of this case is shown in Fig. 5a. Alternatively, in the scenario B, the formed product may desorb and subsequently react along the diffusion path of the zeolite to form larger species that ultimately lead to deactivation. This would imply product desorption and sequential interaction of these products with other surface species, such as other adsorbed products along the diffusion path to form species that do not desorb and deactivate sites. In this scenario, a longer diffusion path (larger crystallite size or higher site density) would promote more rapid deactivation. Scenario C postulates that the adsorbed products sequentially interact with gas phase reactants such as 2-MF before they desorb from the active site where they were formed.

Under conditions depicted here where the partial pressure of the acyl acceptor 2-MF is maintained as constant, the reaction rate is proportional to the coverage of acetic acid on the surface, as shown in Equation (6) and Fig. 2b and 2e, which subsequently converts to form surface acyl species. For simplicity, adsorption of 2-MF and product are not

incorporated within the equation, as the partial pressure of 2-MF is low and constant, and the conversion is maintained at low levels.

Acylation rate(at constant
$$P_{2MF}$$
) $\propto k\theta_{AA} \propto \frac{kK_{AA}P_{AA}}{1 + K_{AA}P_{AA}}$ (6)

We note that prior reports have used TPD studies to suggest that acetic acid is bound to the surface with at least comparable energetics as 2-MF [14], implying that at the high excess concentration of AA, 2-MF direct competition for active sites as depicted in Scenario A will be challenging. To further study the role of site competition, we employ additional species to make this site competition even more challenging to evaluate its relevance in deactivation pathways. Under conditions where the surface is saturated with acetic acid, added non-reactive species that adsorb to surface sites will simply lower acetic acid surface coverage, and therefore lower observed rates, requiring consequential increased partial pressures of acetic acid to compensate and increase the rate to that which was observed without inclusion of these additional non-reactive species. The reaction rate in this case can be described by Equation (7). Adding a non-reactive species (in this case toluene) not only influences reaction rates, but also can modify deactivation as illustrated in Equation (8). The outcome of this will depend heavily on the particular species responsible for deactivation, which could be either adsorbed 2-MF undergoing self-coupling reactions (scenario A or B) or the adsorbed product participating in secondary reactions with gas phase 2-MF (scenario C), as discussed above. P_D in Equation (8) is used to represent this deactivating species, either adsorbed 2-MF or the product Ac-MF. Regardless of the species responsible, it is reasonable to assume that this species is activated over the catalyst and interacts with 2-MF to yield higher molecular weight species that ultimately result in catalyst deactivation.

Acylation rate(at constant
$$P_{2MF}$$
) $\propto k\theta_{AA} \propto \frac{kK_{AA}P_{AA}}{1 + K_{AA}P_{AA} + K_{toluene}P_{toluene}}$ (7)

Assuming the species that ultimately interacts with either a) surface or b) adsorbed species to form larger products that result in catalyst deactivation is equilibrated with the gas phase, the addition of toluene will diminish deactivation rates, as would be the case in scenario A or scenario B in Fig. 5. Scenario C assumes the product is not yet equilibrated with the gas phase and therefore the presence of toluene will not influence deactivation rates.

Deactivation
$$rate \propto k_D \theta_D \propto \frac{k_D K_D P_D P_{2MF}}{1 + K_{AA} P_{AA} + K_{toluene} P_{toluene} + K_D P_D}$$
 (8)

In this case, toluene is employed as a non-reactive species due to its strong binding affinity for Brønsted acid sites as well as the well-established high barrier for the acylation reaction. Toluene is a far inferior acyl acceptor when compared with 2-MF [4,29,30]. When contrasting the ability of toluene to compete for adsorption sites along with 2-MF and AA, we note that the proton affinity (PA) of Toluene is (784 kJ/mol) [31], which is identical value to the PA of AA [14] (784 kJ/mol). Although PA of 2-MF is higher (866 kJ/mol) than both AA and Toluene, it is suggested that adsorption competition can be further

influenced by multiple factors in addition to proton affinity, such as the size of the molecule within the confining environment, hydrogen bonding [14], and other factors that can alter adsorption energetics, which implies that factors in addition to proton affinity influence interactions of various molecules with the active sites [32]. The potential of toluene to compete for sites coupled with the lack of reactivity under these conditions makes toluene a promising candidate to modify surface coverages. Introducing non-reactive compounds is sometimes proposed as a route to mitigate catalyst deactivation rates [33].

The influence of toluene on reaction rates is shown in Fig. 6a, where it is clear that toluene effectively competes with acetic acid and diminishes observed reaction rates as would be expected from Equation (7). It is important to note that the gas phase partial pressure of AA and 2-MF were maintained constant in all cases. Fig. 6b then shows that by further increasing the partial pressure of AA, turnover frequencies consistent with an acid saturated surface are achieved once again. The conditions consisting of a 1:0 vs. 2:0.5 M ratio of AA to toluene are ideal for investigating deactivation reaction pathways. In this instance, following Equation (8), because 2-MF is maintained at an identical partial pressure, the coverage of 2-MF on the surface will be significantly reduced in the latter case where there is the competitive adsorption of

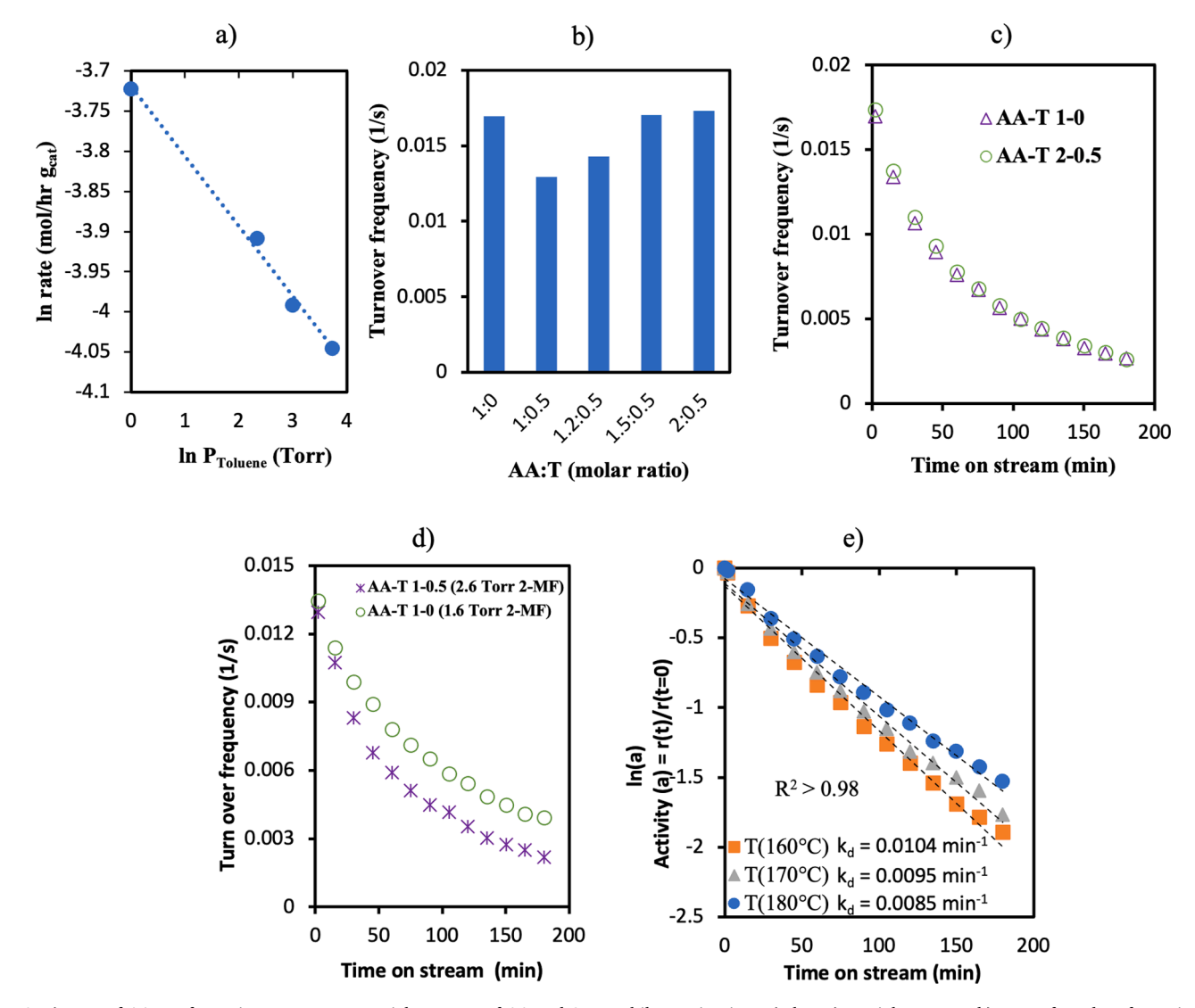


Fig. 6. a) Rate of AA-MF formation at constant partial pressure of AA and 2-MF while varying inert (toluene) partial pressure. b) Rate of product formation at constant 2-MF partial pressure as a function AA and toluene partial pressure. c) contrasting deactivation profiles for two different AA-toluene ratios with constant 2-MF pressure. d) comparing modified partial pressures as a function of 2-MF with two different AA-toluene ratios e) Decay rate and deactivation constants as a functions of reaction temperature. Reactionsconducted over HZSM-5 (Si/Al = 40) at T = 160 °C with $P_{AA} = 40$ torr, $P_{2-MF} = 2.6$ torr, $P_{Toluene} = 0-40$ torr.

toluene, while conversion and turnover frequency is constant. The same experiments were conducted at a higher temperature (240 $^{\circ}$ C) as presented in figures S8a and b, revealing similar behavior when varying toluene and AA molar ratios. However, operating at high temperature toluene begins to participate in the reaction, leading to the formation of acylated toluene products and faster deactivation as illustrated in figure S10 which can be expected since these products are known to lead to sequential oligomerization reactions [24].

Fig. 6c reveals the rate of activity loss as a function of time on stream when comparing two cases with different AA: toluene ratios, where the surface coverage of 2-MF is not the same, but the conversion and TOF in the two cases are equal. Interestingly, a similar deactivation profile exists in these two cases. This illustrates that under conditions where the catalyst surface is saturated by acetic acid, competition for active sites is not a significant contributor to the observed deactivation rates. This contrasts the observations over a non-saturated catalyst surface (Fig. 3) where 2-MF self-coupling reactions clearly enhance deactivation rates. Because scenario A proposes that the competitive adsorption of 2-MF causes catalyst deactivation, the sum of the above observations effectively rules out scenario A in Fig. 5 on an acid saturated surface.

Scenario B implies sequential readsorption of the product as it exits the catalyst pore, which would be a strong function of diffusion path. While sequential reactions along a diffusion path, especially in microporous environments, is a common explanation of deactivation pathways [34] this is unlikely to be a significant cause of catalyst deactivation under the acid saturated conditions reported here. This is supported by the similar observation as discussed above, that any species that desorbs into the gas phase will undergo competition for active sites as it progresses along the diffusion path. The toluene that is introduced will inhibit readsorption of the product Ac-MF along this diffusion path as Equation (8) would suggest and subsequently diminish deactivation rates. Further supporting this argument, reaction rates over a partially Na titrated sample (without adding toluene) Na-ZSM-5 also reveals a lack of correlation between diffusion path and deactivation rates. The measured BAS density is reduced from 0.102 to 0.076 mmol/g upon Na exchange as shown in Figure S12. Fig 1b shows that Na exchange results in similar initial acylation rates per active site as well as identical loss of activity with time on stream. The fact that deactivation rates are identical in the cases depicted in Fig. 6c and Fig 1b suggests that Scenario B is unlikely to play a significant role under these conditions.

Scenario C, where a gas phase molecule interacts with the product prior to desorption is in agreement with the observations depicted here. Therefore, we propose this as the most likely path to deactivation on a fully saturated surface. If deactivation proceeds via the interaction of adsorbed product species and a gas phase molecule, 2-MF is the most likely gas phase deactivating agent considering its concentration. If this were the case, deactivation rates would be a strong function of 2-MF gas phase partial pressure. Fig. 6d illustrates that this is indeed the case, modification of gas phase 2-MF partial pressure also alters reaction rates, so to compensate for this, toluene is added to decrease the AA coverage on the surface such that the initial rates at two different gas phase 2-MF concentrations are equivalent. This implies that the rate of formation of product and therefore the concentration of product is equivalent in the two cases. In this scenario, it is observed that the lower gas phase 2-MF concentration indeed results in diminished deactivation rates over the catalyst surface.

Scenario C should be influenced by the lifetime of product on the surface as well. Accordingly, a faster product desorbing will reduce the probability of the proposed sequential reaction and hence catalyst deactivation, while the rate constant for deactivation would increase as temperature increases. Deprotonation of the adsorbed Wheland intermediate to regenerate the surface acid site, which is the step prior to product desorption is an energetically demanding step and has been referred by some authors as the rate controlling step [12,17]. If the enthalpy of adsorption of the product is greater in magnitude than the

activation energy of sequential reactions of the product with gas phase 2-MF leading to the formation of heavier products, deactivation rates should be less pronounced as temperature is increased. Directly altering the adsorption energy of the formed products, however, would require implementation of a different catalyst with either a different proton affinity or confining environment. Considering the observations from previous studies, the influence of the reaction temperature on catalyst deactivation was tested where obtained results are presented in Fig. 6e. It is clear that the trajectories of the decay rate change with temperature and the deactivation constants decrease as temperature increases, which further supports the relevance of scenario C on deactivation rates as depicted in Fig. 5c.

3.5. Analysis of the sequential reaction products

3.5.1. Soft coke

To decouple the responsible species for the catalyst deactivation, two types of coke were considered and distinguished as soft coke (light oligomers) and hard coke (heavy oligomers). It is intriguing that some of the more prevalent observed species appear to be products of self coupling reactions of furanics. The presence of these two types were recognized and reported by Corma et al. [35]. The soft coke was extracted and analyzed using two different methods. The first method is temperature program sweeping with N2 (TPS-N2) in which the spent catalyst after the acylation reaction was heated from the reaction temperature (160 °C) to 500 °C at a ramp rate of 10 °C/min and held at 500 °C for 1 h in flowing N2. Under these conditions, soft coke is removed from the catalyst pores and was collected and dissolved in a cold n-decane trap. Then, the liquid solution was directly injected and analyzed by a GC-MS. High amounts of retained aromatics and heteroaromatics were observed as shown in Figure S13. As a complementary approach, the spent catalyst was also analyzed in a pyroprobe system. Three different samples were treated under different temperatures (300, 400, and 500 °C). The spectra of evolved species found using this technique in Figures S14a-c is similar to what was found via TPS-N2 in figure S13, which confirms the presence of these light oligomers that are mostly alkylated aromatics. Treatment through TPS-N2 is expected to rejuvenate the active sites in the catalyst by removing and eliminating aromatics and light oligomers. To examine this theory, the spent catalyst (after 3 h TOS at 160 $^{\circ}$ C) was subjected to sweeping in N₂ at either 300 $^{\circ}\text{C}$ or 500 $^{\circ}\text{C}$ for 1 h. At this point, the reactor was cooled down to the reaction temperature at 160 °C prior to reactant reintroduction under the previously stated reactant conditions to assess activity after the sweeping treatment. Interestingly, the reaction only recovered approximately 50 % of the initial rate regardless of the treatment temperature employed as presented in Fig. 7a. This is a similar recovery of activity post N2 sweeping as others have observed upon reacting biomass-derived oxygenates over HZSM-5 [36]. Adsorbed species that do not leave through thermal sweeping alone will continue to become more graphitic and eventually will convert to heavy carbonaceous oligomers, or hard coke [37,38]. When repeating this experiment using a lower site density catalyst (HZSM-5-140) at higher reaction temperature of 240 °C followed by sweeping in inert at 300 °C reveals a nearly identical fractional recovery of activity post N2 sweeping. Consequently, the oligomers produced under these conditions serve as precursors to heavy more graphitic species that require combustion to recover additional activity as will be discussed in the next section.

3.5.2. Hard coke

Unlike soft coke, characterizing heavy oligomers designated as hard coke is a challenging task. In order to precisely evaluate the hard coke, the spent catalyst was pretreated by TPS-N $_2$ at 500 $^{\circ}$ C for 1 h to selectively remove the soft coke while maintaining the hard coke in the spent catalyst. Characterization techniques such FT-IR spectroscopy and TGA have been implemented. Additionally, nitrogen adsorption analysis and IPA-TPRx on the spent catalyst samples were conducted to elucidate the

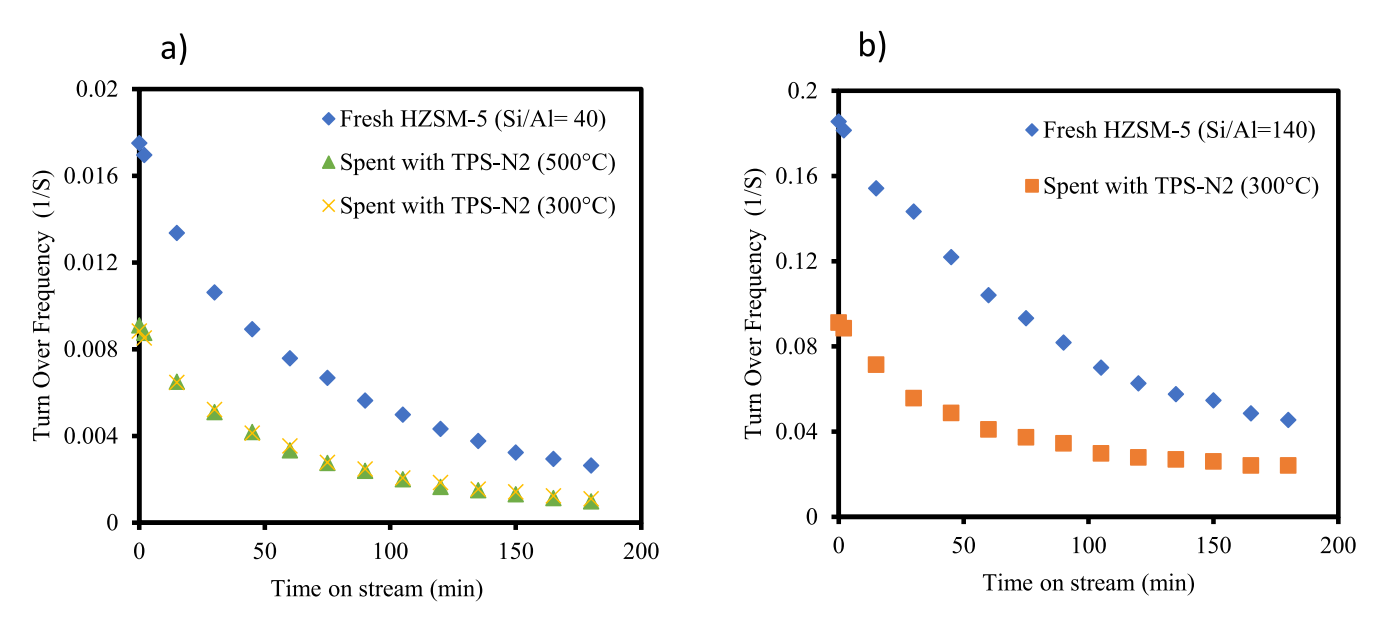


Fig. 7. a) Comparison between rate of acylation $P_{AA} = 40$ torr, $P_{2\text{-MF}} = 2.6$ torr at $160\,^{\circ}\text{C}$ on fresh and spent HZSM-5 (Si/Al = 40) catalyst with TPS-N₂ at different treatment temperatures $300\,^{\circ}\text{C}$ and $500\,^{\circ}\text{C}$ under flowing N_2 (125 SCCM). b) Comparison between rate of acylation $P_{AA} = 40$ torr, $P_{2\text{-MF}} = 2.6$ torr at 240 $^{\circ}\text{C}$ on fresh and spent HZSM-5 (Si/Al = 140) catalyst with TPS-N₂ at 300 $^{\circ}\text{C}$ under flowing N_2 (125 SCCM).

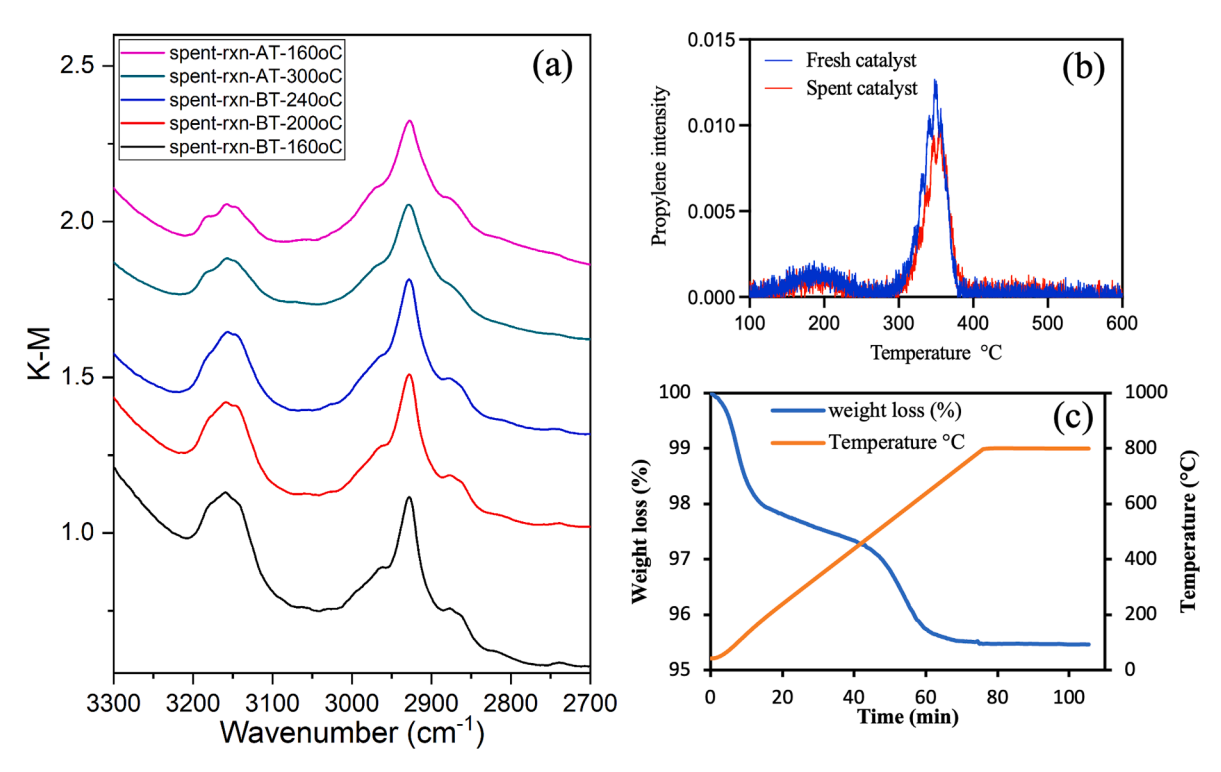


Fig. 8. Hard coke analysis (a) Evolution of IR spectra of spent HZSM-5Si/Al = 40 as a function of temperature (BT = before treatment at 300 °C, AT = after treatment at 300 °C). Spectra are offset for clarity. (b) Propylene signals resulted from IPA-TPRx of fresh and spent HZSM-5 (Si/Al = 40) catalyst samples used for BAS density quantification (c) Estimating the mass of hard coke using TPO-TGA of spent HZSM-5 (Si/Al = 40) catalyst after TPS-N₂.

influence of hard coke on the physiochemical properties.

Fig. 8a shows the common regions of vibration in the FTIR spectra of the hard coke deposits on the spent HZSM-5 after acylation. The spectra region 3200–2700 cm $^{-1}$ corresponds to vibrations associated with olefins and aromatics [38,39], which can be observed before and after temperature treatment under flowing helium. The deconvoluted IR spectra in figure S15 reveals prominent CH_2 and CH_3 stretching in 3 peaks at 2960, 2930, and 2870 cm $^{-1}$ assigned to olefins while C—H band stretching at 3155 cm $^{-1}$ can be ascribed to aromatics and alkylated

aromatics. These IR vibrations of olefins and aromatics of the coke in the spent catalyst match those in literature for biomass conversion [40]. The stretching regions found in IR spectra coincide with the species analyzed by GC–MS using TPS-N₂ and pyroprobe presented in figures \$13,14a-c.

The loss of activity found in Fig. 7a, b even after high temperature treatment under flowing N_2 is attributed to the loss of BAS caused by heavy coke deposits. IPA-TPRx was used to quantify BAS densities both fresh and spent catalysts as illustrated in Fig. 8b with a noticeably lower propylene peak in the spent catalyst. BAS density was quantified by

calculating the area under the curves giving 0.394 and 0.327 mmol/g for the fresh and spent HZSM-5 catalyst, respectively. These losses could be ascribed to both active sites that are covered with large unsaturated hydrocarbons as well as pore blockage that limits accessibility to active sites. The total pore volume (and micropore volume) of the zeolite was measured by using the classical single-point method of converting the total measured gas quantity adsorbed into a liquid quantity, assuming that the adsorbate density is the same as bulk liquid nitrogen. The Horvath-Kawazoe method was used to estimate the micropore volume—which showed about a 30 % difference between the spent and fresh catalysts (0.14 mL/g vs 0.18 mL/g, respectively), which is similar to the trend observed for the total pore volume (0.20 mL/g vs 0.26 mL/g). The greater reduction in rate after inert sweeping in Fig. 7a and 7b (~50 %) when contrasted with the more modest loss in BAS density via IPA TPRx could be explained by either a) partial pore blockage that

impede access of bulky acylation reactants and products or b) selective deactivation of sites with higher intrinsic activity. Acid site characterization is carried out under conditions such that sufficient time is given to ensure that isopropylamine is able to diffuse to all accessible Bronsted acid sites. Therefore, pore narrowing due to carbon deposits or other features that may slow diffusion of larger molecules may still be counted as active sites via this technique. We speculate that this is the primary cause of the discrepancy. Further in support of argument (a) above this is the similar reduction in TOF reported for the two zeolites with different concentrations in active sites. The MFI 140 zeolite, given its low Al content is generally assumed to have isolated sites at intersections, so a significant fraction of highly active sites that are preferentially titrated as presumed in (b) is unlikely. The amount of heavy coke accumulated in the spent catalyst was calculated via burning the hydrocarbons via TGA in a flowing stream containing oxygen, and evaluating the weight loss

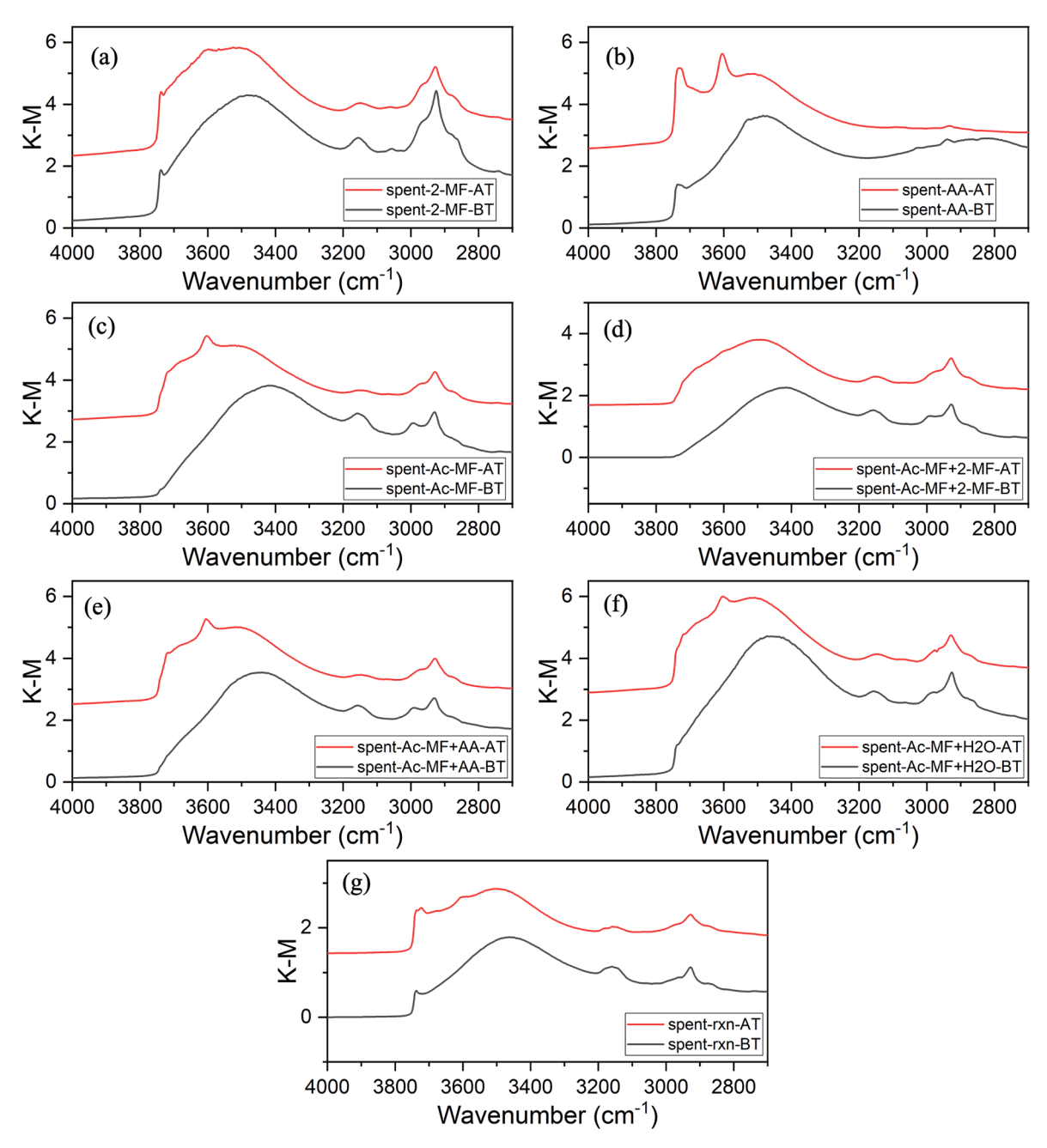


Fig. 9. FTIR spectroscopy of HZSM-5 (Si/Al = 40) at 160 °C before treatment (BT) and after treatment at 300 °C under flowing helium (AT) of spent catalyst after exposure of (a) 2-MF only for 60 min, (b) AA only for 60 min, (c) Ac-MF only for 60 min, (d) Ac-MF for 30 min followed by 2-MF for 30 min, (e) Ac-MF for 30 min followed by AA for 30 min, (f) Ac-MF for 30 min followed by water for 30 min, (g) Normal reaction conditions (rxn) for 3 h. Spectra are offset for clarity.

from the sample. Fig. 8c demonstrates the weight % loss progress as temperature increases resulting a loss of 4.5 wt% of the total mass of spent catalyst.

3.5.3. Specific contributions of reactants and products to coke formation

Although the loss of activity due to direct contact of involved chemical species has been discussed previously, it is constructive to examine the surface of the catalyst after exposure to each participating molecule to correlate surface species with the reaction behavior described above. During this acylation reaction, there are 4 relevant species, two reactants (AA and 2-MF) and two products (Ac-MF and water). Therefore, 6 scenarios were investigated that could lead to coke formation on the surface of clean catalyst particles by directly introducing the involved chemical species at the standard reaction temperature (160 °C). Fig. 9a-f reflect the FTIR spectra of spent HZSM-5 (Si/Al = 40) catalysts for each scenario and is contrasted to Fig. 9g for FTIR analysis of the spent catalyst collected after a typical acylation reaction. The peak intensities for the C—H vibrations in the regions of 3200–2700 cm⁻¹ correspond to the scale of the coke generated for each scenario while the O—H vibrations in the 3600 cm⁻¹ reflect the Brønsted acid sites [22]

To this point, 2-MF alone undoubtedly forms large amounts of coke on the catalyst surface and leads to major losses in activity. Fig. 9a, indicates that heavy oligomers are relatively preserved even after high temperature (300 $^{\circ}$ C) treatment and consequently minimize active site recovery. Unlike 2-MF, oligomerization due to AA extended exposure is negligible. In fact, Fig. 9b illustrates how heating up the catalyst under flowing helium regenerates nearly all the BAS. This aligns with previous findings in Fig. 3 where it was shown how it takes several hours of AA feeding to observe significant losses in activity of the zeolite.

We proposed that under extremely high ratio of AA to 2-MF, AA will limit 2-MF absorption and limit its ability interact directly with BAS, and the product (Ac-MF), which arrives on the surface through 2-MF interaction with surface acyl species would become the more significant major coke precursor. This can occur through Ac-MF self-oligomerization, or Ac-MF interaction with the other involved species (2-MF, AA, or water). Self-oligomerization would require Ac-MF products to either migrate along the surface or equilibrate with the gas phase and somehow contribute significantly to deactivation rates by interacting with adsorbed species. We hypothesize that this pathway is unlikely due to the much lower partial pressure of the products when contrasted with the 2-MF feed itself, which may similarly interact with adsorbed products. Fig. 9c suggests that the adsorption of the product itself indeed forms some features representing olefinic species in regions located at 2960, 2930, 2870 cm^{-1} , as well as aromatic species at 3155 cm^{-1} . However, after mild temperature treatment those peaks alleviate including a major reduction in the aromatic peak region resulting a significant growth in the O—H stretching peak at the 3600 cm⁻¹ and hence a major BAS regeneration. Similar effects were observed in Fig. 9e, f when adsorbed Ac-MF was exposed to AA or water, which suggests that these chemical species do not contribute to sequential reactions to the same irreversible extent as those that are kinetically relevant contributors to the deactivation rates observed during acylation reactions. On the other hand, when mimicking the proposed deactivation mechanism in Fig. 5c via introducing 2-MF to a surface saturated with Ac-MF, this results in large carbonous species that show minimal removal from the catalyst surface even after elevated temperature treatment as illustrated in Fig. 9d. Additionally, BAS recovery was negligible as opposed to the ability of active site regeneration in scenarios when exposing AA or water to adsorbed Ac-MF. The scenario in Fig. 9d show similar minimal BAS recovery when compared with a typical acylation reaction in Fig. 9g, which suggests the predominant mode of deactivation under acylation reaction conditions on an acid saturated surface does indeed result from 2-MF interacting with adsorbed products, in alignment with the conclusions inferred by modifying surface coverages of various species in prior sections.

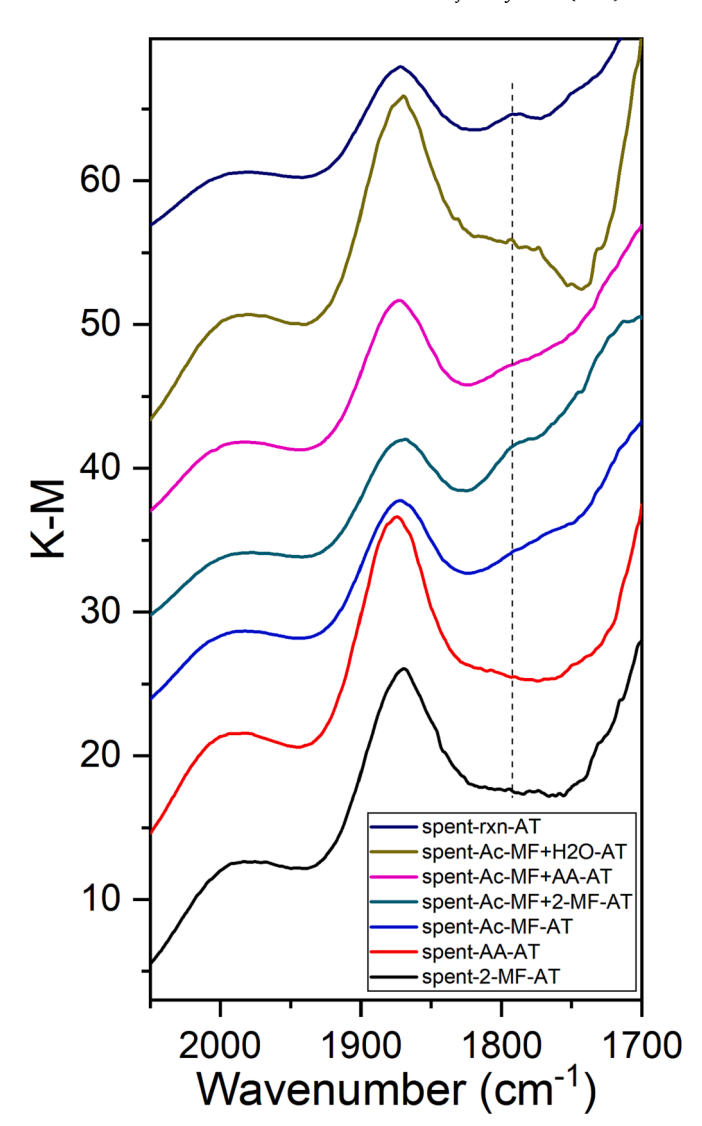


Fig. 10. FTIR spectroscopy of spent HZSM-5 (Si/Al = 40) at 160 °C after temperature treatment at 300 °C under flowing helium (AT) of spent catalyst after exposure of, 2-MF only for 60 min (spent-2-MF-AT), AA only for 60 min (spent-AA-AT), Ac-MF for 30 min (spent-Ac-MF-AT), Ac-MF for 30 min followed by 2-MF for 30 min, (spent-Ac-MF + 2-MF-AT), Ac-MF for 30 min followed by AA for 30 min (spent-Ac-MF + AA-AT), Ac-MF for 30 min followed by water for (spent-Ac-MF + H2O-AT), Normal reaction conditions (rxn) for 3 h (spent-rxn-AT). A line to highlight the feature in the C—O bond stretching region is added to all spectra. Spectra are offset for clarity.

Implementing the scenarios shown in Fig. 9 using FTIR spectroscopy solidify the argument of shifting catalyst the deactivation mechanism from 2-MF self-coupling at low AA coverage to sequential reactions between adsorbed Ac-MF surface species prior to desorption and gas phase 2-MF at high AA coverage as discussed previously in Fig. 2. As further contrasting the IR spectra in all scenarios in Fig. 9, a common peak in the 1800 cm⁻¹ region in Fig. 10 corresponds to C=O stretching [41] was observed in both scenario created by flowing 2-MF on adsorbed Ac-MF, as well as the spent catalyst after normal acylation reaction on an acid saturate surface. Such a peak suggests a mutual heavy oligomer is produced when a sequential reaction occurs between gas phase 2-MF and adsorbed Ac-MF product.

4. Conclusion

This study reveals the pathways responsible for catalyst deactivation during Friedel Crafts acylation under conditions where the surface is saturated with the acylating agent, where deactivation mechanisms have not been previously studied. At low AA surface coverages, direct 2-MF interactions with available Brønsted acid sites lead to rapid coke forming reactions. As acid concentrations are increased and the surface becomes saturated with carboxylic acids and surface acyl species, deactivation rates are markedly reduced. Under saturated conditions, however, deactivation still persists. By manipulating surface coverage and introducing strongly binding species that does not participate in the reaction, it is revealed that the pathway responsible for deactivation under saturated surface conditions shifts to interactions of adsorbed products with gas phase 2-MF species. Direct competition of 2-MF with the catalyst surface no longer significantly contributes to deactivation rates under these conditions. Readsorption and reaction of produced products along the diffusion path similarly do not contribute to observed rate losses under these conditions. Deactivation rates can therefore be mitigated simply by altering the gas phase partial pressure of the highly reactive acyl acceptors, or by altering the adsorption energy and therefore lifetime of products to decrease the probability of reaction prior to desorption from the active sites. These results reveal a blueprint for further extending the lifetime of Friedel Crafts catalysts upon employing highly reactive acyl acceptors.

Funding

The authors are grateful for funding from NSF grants 1653935 and 2029394. IA acknowledges support from the Saudi Arabian Cultural Mission (SACM) for partial funding of his graduate studies.

Declaration of Competing Interest

The authors declare that they have no known competing financial interests or personal relationships that could have appeared to influence the work reported in this paper.

Data availability

Data will be made available on request.

Acknowledgement

The authors are thankful for assistance with the TGA studies by Ana Jerdy, Erich Metzger for assistance with the fast pyrolysis studies, and Andrew D'Amico for his assistance with the pore volume measurements.

Appendix A. Supplementary material

Supplementary data to this article can be found online at https://doi.org/10.1016/j.jcat.2023.07.009.

References

- [1] G. Sartori, R. Maggi, Chem. Rev. 106 (2006) 1077-1104.
- [2] G.A. Olah, Friedel-crafts chemistry, in: Across Conventional Lines: Selected Papers of George A Olah Volume 1, World Scientific, 2003, pp. 119-121.

- [3] S. Dasgupta, B. Torok, Curr. Org. Synth. 5 (2008) 321-342.
- [4] A. Gumidyala, B. Wang, S. Crossley, Sci. Adv. 2 (2016) e1601072.
- [5] D.S. Park, K.E. Joseph, M. Koehle, C. Krumm, L. Ren, J.N. Damen, M.H. Shete, H. S. Lee, X. Zuo, B. Lee, W. Fan, D.G. Vlachos, R.F. Lobo, M. Tsapatsis, P. J. Dauenhauer, ACS Cent. Sci. 2 (2016) 820–824.
- [6] G.G. Zaimes, A.W. Beck, R.R. Janupala, D.E. Resasco, S.P. Crossley, L.L. Lobban, V. Khanna, Energ, Environ. Sci. 10 (2017) 1034–1050.
- [7] A.W. Beck, A.J. O'Brien, G.G. Zaimes, D.E. Resasco, S.P. Crossley, V. Khanna, ACS Sustain. Chem. Eng. 6 (2018) 5826–5834.
- [8] J.A. Herron, T. Vann, N. Duong, D.E. Resasco, S. Crossley, L.L. Lobban, C. T. Maravelias, Energ. Technol. 5 (2017) 130–150.
- [9] N.N. Duong, B. Wang, T. Sooknoi, S.P. Crossley, D.E. Resasco, ChemSusChem 10 (2017) 2823–2832.
- [10] S. Gutiérrez-Rubio, M. Shamzhy, J. Čejka, D. Serrano, I. Moreno, J. Coronado, Appl. Catal. B 285 (2021), 119826.
- [11] M. Koehle, E. Saraçi, P. Dauenhauer, R.F. Lobo, ChemSusChem 10 (2017) 91-98.
- [12] M. Koehle, Z. Zhang, K.A. Goulas, S. Caratzoulas, D.G. Vlachos, R.F. Lobo, Appl. Catal. A 564 (2018) 90–101.
- [13] S.K. Green, R.E. Patet, N. Nikbin, C.L. Williams, C.-C. Chang, J. Yu, R.J. Gorte, S. Caratzoulas, W. Fan, D.G. Vlachos, Appl. Catal. B 180 (2016) 487–496.
- [14] Y. Ji, J. Pan, P. Dauenhauer, R.J. Gorte, Appl. Catal. A 577 (2019) 107-112.
- [15] D.S. Park, K.E. Joseph, M. Koehle, C. Krumm, L. Ren, J.N. Damen, M.H. Shete, H. S. Lee, X. Zuo, B. Lee, ACS Cent. Sci. 2 (2016) 820–824.
- [16] T.V. Bui, S. Crossley, D.E. Resasco, C-C coupling for biomass-derived furanics upgrading to chemicals and fuels, in, Wiley-VCH Verlag and Co, KGaA (2016) 431–494
- [17] T.-H. Chen, D.G. Vlachos, S. Caratzoulas, ACS Catal. 11 (2021) 9916-9925.
- [18] F. Schüth, M.D. Ward, J.M. Buriak, Common pitfalls of catalysis manuscripts submitted to chemistry of materials, in, ACS Publications, 2018.
- [19] R. Koros, E. Nowak, Chem. Eng. Sci. 22 (1967) 470.
- [20] R.J. Madon, M. Boudart, Ind. Eng. Chem. Fundam. 21 (1982) 438-447.
- [21] T.N. Pham, V. Nguyen, B. Wang, J.L. White, S. Crossley, ACS Catal. 11 (2021) 6982–6994.
- [22] T.N. Pham, V. Nguyen, H. Nguyen-Phu, B. Wang, S. Crossley, ACS Catal. 13 (2023) 1359–1370.
- [23] K. Chen, M. Abdolrahmani, S. Horstmeier, T.N. Pham, V.T. Nguyen, M. Zeets, B. Wang, S. Crossley, J.L. White, ACS Catal. 9 (2019) 6124–6136.
- [24] P. Botella, A. Corma, J. López-Nieto, S. Valencia, R. Jacquot, J. Catal. 195 (2000) 161–168.
- [25] C. Padro, C.R. Apesteguía, Catal. Today 107 (2005) 258-265.
- [26] I. Neves, F. Jayat, P. Magnoux, G. Perot, F. Ribeiro, M. Gubelmann, M. Guisnet, J. Mol. Catal. 93 (1994) 169–179.
- [27] F. Jayat, M. Guisnet, M. Goldwasser, G. Giannetto, Acylation of phenol with acetic acid. Effect of density and strength of acid sites on the properties of MFI metallosilicates, in: Studies in Surface Science and Catalysis, Elsevier, 1997, pp. 1149–1156.
- [28] A.D. Chowdhury, J. Gascon, Angew. Chem. Int. Ed. 57 (2018) 14982–14985.
- [29] M. Bejblova, D. Prochazkova, J. Čejka, ChemSusChem: Chem. Sustain. Energy Mater. 2 (2009) 486–499.
- [30] H.K. Chau, D.E. Resasco, P. Do, S. Crossley, J. Catal 406 (2022) 48–55.
- [31] C. Wang, S. Li, X. Mao, S. Caratzoulas, R.J. Gorte, Catal. Lett. 148 (2018) 3548–3556.
- [32] R.J. Gorte, S.P. Crossley, J. Catal. 375 (2019) 524-530.
- [33] K.P. Vinter, P.J. Dauenhauer, Cat. Sci. Technol. 8 (2018) 3901–3909.
- [34] S. Wan, C. Waters, A. Stevens, A. Gumidyala, R. Jentoft, L. Lobban, D. Resasco, R. Mallinson, S. Crossley, ChemSusChem 8 (2015) 552–559.
- [35] A. Corma, C. Martínez, E. Doskocil, J. Catal. 300 (2013) 183–196.
- [36] P.T. Williams, P.A. Horne, Fuel 74 (1995) 1839-1851.
- [37] A.T. Aguayo, A.G. Gayubo, J. Ereña, A. Atutxa, J. Bilbao, Ind. Eng. Chem. Res. 42 (2003) 3914–3921.
- [38] M. Díaz, E. Epelde, J. Valecillos, S. Izaddoust, A.T. Aguayo, J. Bilbao, Appl Catal B 291 (2021), 120076.
- [39] E. Epelde, M. Ibañez, A.T. Aguayo, A.G. Gayubo, J. Bilbao, P. Castaño, Microporous Mesoporous Mater. 195 (2014) 284–293.
- [40] B. Valle, P. Castaño, M. Olazar, J. Bilbao, A.G. Gayubo, J. Catal. 285 (2012) 304–314.
- [41] B. Bachiller-Baeza, J. Anderson, J. Catal. 228 (2004) 225-233.